Immunity
Article

Antibody Light-Chain-Restricted Recognition of the Site of Immune Pressure in the RV144 HIV-1 Vaccine Trial Is Phylogenetically Conserved

Kevin Wiehe,[1,11,*] David Easterhoff,[1,11] Kan Luo,[1,11] Nathan I. Nicely,[1] Todd Bradley,[1] Frederick H. Jaeger,[1] S. Moses Dennison,[1] Ruijun Zhang,[1] Krissey E. Lloyd,[1] Christina Stolarchuk,[1] Robert Parks,[1] Laura L. Sutherland,[1] Richard M. Scearce,[1] Lynn Morris,[2] Jaranit Kaewkungwal,[3] Sorachai Nitayaphan,[4] Punnee Pitisuttithum,[3] Supachai Rerks-Ngarm,[5] Faruk Sinangil,[6] Sanjay Phogat,[7] Nelson L. Michael,[8] Jerome H. Kim,[8] Garnett Kelsoe,[1] David C. Montefiori,[1] Georgia D. Tomaras,[1] Mattia Bonsignori,[1] Sampa Santra,[9] Thomas B. Kepler,[10] S. Munir Alam,[1] M. Anthony Moody,[1] Hua-Xin Liao,[1] and Barton F. Haynes[1,*]

[1]Duke Human Vaccine Institute, Duke University School of Medicine, Durham, NC 27710, USA
[2]National Institute for Communicable Diseases, Johannesburg 2131, SA and the Centre for the AIDS Programme of Research in South Africa (CAPRISA)
[3]Department of Tropical Medicine, Mahidol University, Bangkok 10400, Thailand
[4]Armed Forces Research Institute of Medical Sciences (AFRIMS), Bangkok 10400, Thailand
[5]Department of Disease Control, Ministry of Public Health, Nonthaburi 11000, Thailand
[6]Sanofi Pasteur, Inc., Swiftwater, PA 18370, USA
[7]Global Solutions for Infectious Diseases, South San Francisco, CA 94080, USA
[8]US Military Research Program, Walter Reed Army Institute of Research, Silver Spring, MD 20910, USA
[9]Beth Israel Deaconess Medical Center, Harvard University School of Medicine, Boston, MA 02215, USA
[10]Department of Microbiology, Boston University, Boston, MA 02118, USA
[11]Co-first author
*Correspondence: kevin.wiehe@dm.duke.edu (K.W.), barton.haynes@dm.duke.edu (B.F.H.)
http://dx.doi.org/10.1016/j.immuni.2014.11.014

SUMMARY

In HIV-1, the ability to mount antibody responses to conserved, neutralizing epitopes is critical for protection. Here we have studied the light chain usage of human and rhesus macaque antibodies targeted to a dominant region of the HIV-1 envelope second variable (V2) region involving lysine (K) 169, the site of immune pressure in the RV144 vaccine efficacy trial. We found that humans and rhesus macaques used orthologous lambda variable gene segments encoding a glutamic acid-aspartic acid (ED) motif for K169 recognition. Structure determination of an unmutated ancestor antibody demonstrated that the V2 binding site was preconfigured for ED motif-mediated recognition prior to maturation. Thus, light chain usage for recognition of the site of immune pressure in the RV144 trial is highly conserved across species. These data indicate that the HIV-1 K169-recognizing ED motif has persisted over the diversification between rhesus macaques and humans, suggesting an evolutionary advantage of this antibody recognition mode.

INTRODUCTION

The RV144 vaccine trial showed an estimated vaccine efficacy of 31% (Rerks-Ngarm et al., 2009), and a molecular sieve analysis of breakthrough infections demonstrated 48% vaccine efficacy when the second variable region (V2) of the infecting virus envelope (Env) matched the vaccine Env at lysine (K) at position 169 (Rolland et al., 2012). Isolation of V2 monoclonal antibodies (mAbs) from vaccinees demonstrated that in four V2 antibodies that recognized K169, all light chain second complementarity determining regions (LCDR2) contained a glutamic acid-aspartic acid (ED) motif, and crystal structures of two K169-reactive human mAbs, CH58 and CH59, demonstrated salt bridges formed with K169 by the E of CH58 and the D of CH59 (Liao et al., 2013). Of the four V2 antibodies initially isolated from RV144 vaccinees, mAb CH58 utilized lambda light chain V gene segment 6-57 (*IGLV6-57*) and mAb CH59 utilized *IGLV3-10*, both of which have a germline-encoded ED motif (Lefranc, 2001). Two additional V2 K169 antibodies, HG107 and HG120, independently isolated from RV144 vaccinees also expressed IGLV3-10 light chains and retained the LCDR2 ED motif (Liao et al., 2013). These observations raised the hypothesis that V_λ gene segments carrying the LCDR2 ED motif were required to recognize the HIV-1 V2 K169 epitope and exert the selective pressure apparent in the RV144 vaccine trial (Liao et al., 2013).

Rhesus macaques have been useful models of retrovirus infection pathogenesis as well as for evaluation of protective capacity of antibodies against simian immunodeficiency virus (SIV) and simian-human immunodeficiency virus (SHIV) infections. Study of the rhesus macaque genome has demonstrated that humans and rhesus macaques share ~93% of genome homology (Gibbs et al., 2007), with a common ancestor estimated at ~32 million years ago (Perelman et al., 2011). Thus, study of the rhesus antibody repertoire as a model for how humans will respond to pathogens and vaccines might be a useful approach for the prediction of human antibody responses.

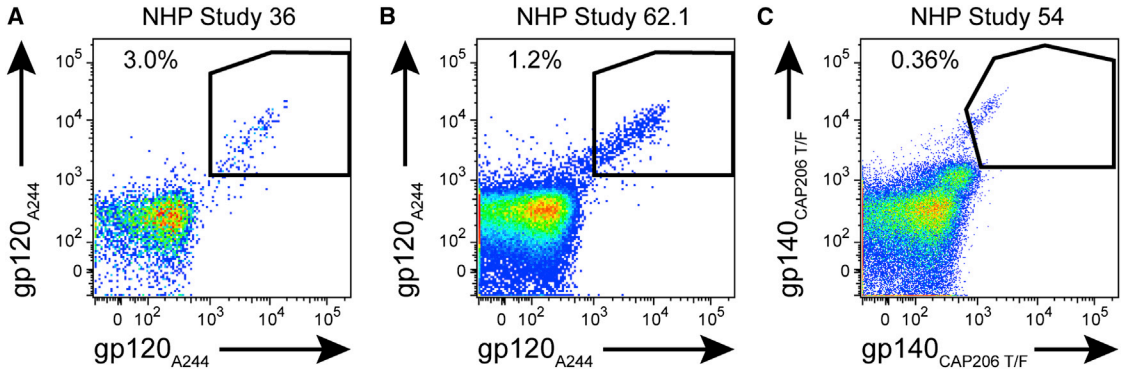

Figure 1. Antigen-Specific Memory B Cell Sorts on Peripheral Mononuclear Blood Cells from Three Nonhuman Primate Studies

Live $CD14^-CD16^-CD20^+CD3^-IgD^-CD27^+$ cells were stained with antigens conjugated to two different fluorophores. Double-positive antigen-specific cells were single-cell sorted into 96-well PCR plates for RT-PCR. AE.A244 gp120-specific memory B cells were (A) 3.0% of NHP study 36 and (B) 1.2% of NHP study 62. NHP study 53 (C) was sorted with CAP206 T/F gp140 and 0.36% of cells were specific for this HIV-1 envelope. Data are representative results of at least three independent experiments.

One route to improvement on the results of the RV144 vaccine trial is to determine whether any V_L genes other than *IGLV6-57* and *IGLV3-10* can be used to target the K169 V2 region. To address this question, we immunized rhesus macaques with the RV144 vaccine Env, AE.A244 gp120, and isolated 27 antibodies that are dependent on V2 K169 for binding to HIV-1 Env gp120. We found that all 27 antibodies utilized the rhesus ortholog of human *IGLV3-10*, i.e., the rhesus *IGLV3-17* gene segment that contains a germline-encoded LCDR2 ED motif. Two additional antibodies were isolated from rhesus immunizations with clade C Envs that recognized V2 K169 that were not IGLV3-17, but rather had ED motifs derived from LCDR2 somatic mutations. Thus, the only observed mechanism of recognition of K169 in primates is via antibodies with lambda light chains with a LCDR2 ED motif. That this germline-encoded rhesus IGLV3-17 and human IGLV3-10 light chain mode of recognition of V2 K169 has persisted through the divergence of humans and rhesus macaques suggests that the V_λ LCDR2 ED motif confers a strong fitness advantage.

RESULTS

Restricted Utilization of Rhesus Macaque IGLV3-17 in Recognition of HIV-1 Env V2 K169

We immunized rhesus macaques with the RV144 vaccine trial Env AE.A244 gp120 in two regimens, one with the same immunogens used in the RV144 trial (Rerks-Ngarm et al., 2009) (NHP study 36; Figure S1A available online), and the other with a heterologous prime-boost strategy with RV144 AE.A244 gp120 Env glycoprotein immunogen as a prime, followed sequentially by AE.427299 gp120, B.9021 gp140, AE.A244 gp120, and then a final boost of AE.A244 and AE.427299 gp120s (NHP study 62.1; Figure S1B). Env proteins 92TH023 gp120 and CM244 gp120 in NHP study 36 and AE.A244 gp120 in NHP study 62.1 included K169 in their V2 loops whereas Env proteins MN.3 gp120 in NHP study 36 and AE.427299 gp120 and B.9021 gp140 in NHP study 62.1 did not (Gnanakaran et al., 2010; Liao et al., 2013).

We isolated antibodies from immunized monkeys utilizing antigen-specific memory B cell sorts with fluorophore-labeled AE.A244 gp120 (Bonsignori et al., 2012) or similarly labeled AE.A244 V1V2 tags protein (Liao et al., 2013) (Figure 1). A total of 39 antibodies were isolated that bound to the V2 region of Env (^{165}LRDKKQKVHALFYKLDIVPIED^{186}) in ELISA assays from NHP studies 36 and 62.1 (Tables S1 and S2). Of the 39 V2-targeted antibodies, 27 antibodies bound at K169 (the site of immune pressure in the RV144 vaccine efficacy trial) as established by alanine scanning binding ELISA assays (Table S1). All 27 V2 K169-dependent antibodies utilized *IGLV3-17* genes with an ED motif in the LCDR2 (Table S2).

Next, we selected a set of 18 V2-reactive antibodies with an ED motif for production in bulk and further characterization. Extensive epitope mapping by alanine-scanning mutagenesis with a 19-residue AE.A244 V2 peptide (^{165}LRDKKQKVHALFYKL DIVPIED^{186}) confirmed that all 18 ED motif-containing antibodies demonstrated K169-dependent binding (Table 1, Figure S2). All antibodies also had H173 as an epitope component and additionally had combinations of K171, F176, Y177, and D180 amino acids in their epitopes. The epitopes recognized by the rhesus antibodies were most similar to the epitope utilized by the previously described human mAb, CH59, derived from an RV144 vaccinee (Liao et al., 2013).

We then characterized the neutralization breadth of the 18 K169-recognizing, ED motif antibodies by using both TZM-bl and A3R5 HIV-1 neutralization assays (McLinden et al., 2013; Sarzotti-Kelsoe et al., 2014). All 18 antibodies neutralized the easy-to-neutralize tier 1 virus AE.92TH023.6 in the TZM-bl assay (Table S3) but failed to neutralize the tier 1 HIV-1 isolate MN.3 (which does not have a K at position 169) and difficult-to-neutralize tier 2 HIV-1 isolate AE.CM244 in TZM-bl. All but one antibody failed to neutralize any HIV-1 isolates tested in the A3R5.7 cell assay (Table S3).

We next confirmed the ED motif as critical to V2 recognition by making single (D51A)- and double (E50A+D51A)-alanine mutations by site-directed mutagenesis to antibody 1518, a separate rhesus antibody from NHP 36 that was not included in the characterization above. Binding to AE.A244 gp120, V1V2 tags, and V2 peptide was reduced for the single-alanine mutant and greatly reduced for the double-alanine mutant (Table S1B).

Table 1. V2 Epitopes of Selected Antibodies

Antibody	Species	V_H	V_L	V2 Epitope
1678	rhesus	3-SC11	λ3-17	K169*, H173, F176, Y177
1697	rhesus	3-SC11	λ3-17	K169*, H173, F176, Y177
1811	rhesus	3-SC11	λ3-17	K169*, H173, D180
1410	rhesus	4-48	λ3-17	K169*, H173, D180
1825	rhesus	4-48	λ3-17	K169*, H173
2552	rhesus	4-48	λ3-17	K169*, H173
975	rhesus	4-79	λ3-17	K169*, K171, H173, Y177, D180
1447	rhesus	4-79	λ3-17	K169*, H173, Y177, D180
1601	rhesus	4-79	λ3-17	K169*, H173, D180
1671	rhesus	4-79	λ3-17	K169*, H173
1819	rhesus	4-79	λ3-17	K169*, H173, Y177
1823	rhesus	4-79	λ3-17	K169*, H173, Y177, D180
1824	rhesus	4-79	λ3-17	K169*, H173, Y177, D180
2553	rhesus	4-79	λ3-17	K169*, H173, D180
2536	rhesus	4-96	λ3-17	K169*, H173, D180
2547	rhesus	4-96	λ3-17	K169*, H173, F176
2653	rhesus	4-96	λ3-17	K169*, H173, D180
2548	rhesus	4-SC6	λ3-17	K169*, H173, D180
1056[a]	rhesus	3-SC11	λ3-SC4	K169*, K171, H173, F176, Y177, D180
1534[a]	rhesus	3-SC11	λ3-SC4	K169*, K171, H173, F176, Y177, D180
CH58[b]	human	5-51	λ6-57	K168, K169*, K171, H173, F176, Y177, K178, D180, P183
CH59[b]	human	3-9	λ3-10	K169*, H173, F176, Y177, D180
HG107[b]	human	3-9	λ3-10	K169*, K171, H173, F176, Y177, D180
HG120[b]	human	3-23	λ3-10	K169*, H173, F176, Y177, D180

V2 epitope residues were defined as residues where EC50 relative to WT for alanine mutations was reduced by >50% in ELISA assay. Epitope positions determined by ELISA were also confirmed by SPR for representative set of mutations (same as listed below). K169, the site of immune pressure in the RV144 trial, is indicated with an asterisk (*).

[a]Antibody footprints mapped by SPR only for mutations K168A, K169A, K171A, H173A, F176A, Y177A, and D180A.

[b]Antibody footprints previously described (Liao et al., 2013).

Additionally, neutralization of AE.92TH023 was lost for all three mutants (Table S3). Taken together, these data demonstrate that the ED motif was essential for recognition of the V2 loop and mediation of neutralization.

The predominance of ED motif-containing antibodies in the V2 response suggested that the V2 is strongly antigenic for naive B cell receptors utilizing IGLV3-17. We computationally inferred the initial V(D)J rearrangements of three representative IGLV3-17, ED-motif-containing antibody clonal lineages (Kepler, 2013) and recombinantly produced them for characterization. All three unmutated common ancestor (UCA) antibodies demonstrated binding to AE.A244 V1V2 tags protein with binding of two of the three UCAs reduced relative to the corresponding mutated antibodies (Table S1C). No neutralization was observed for the three UCAs (Table S3), demonstrating that the neutralization capacity of IGLV3-17 V2 antibodies is not attained until additional mutations are acquired from affinity maturation.

Acquisition of LCDR2 ED Motif via Affinity Maturation

We next asked whether we could observe examples of V2 K169 antibodies induced without the utilization of the CDRL2 ED motif encoding *IGLV3-17* gene from regimens from other NHP studies. For this analysis we isolated antibodies from a rhesus macaque that was immunized with three clade C (CAP206) Envs that each had a lysine at position 169 in V2 (NHP Study 54, Figure S1C). We isolated two antibodies (1056 and 1534) that bound AE.A244 V2 peptide that were dependent for their binding on K169 (Table 1 and Figure S2) and had an ED motif in LCDR2. However, these two antibodies did not use *IGLV3-17*, but rather used the *IGLV3-SC4* gene segment that encodes a KD amino acid pair in the germline LCDR2 (Figure 2A). This K50E mutation in the 1056 and 1534 antibodies was probably the result of VJ hypermutation in germinal centers.

We next asked whether the K50E mutation resulted in improved Env binding. We used site-directed mutagenesis to revert E50 in the LCDR2s of antibodies 1056 and 1534 back to K. Indeed, we found that binding to the CAP206 transmitted-founder gp140 improved 4- to 6-fold for the ED-bearing 1056 and 1534 antibodies compared to 1056 and 1534 E50K reversion mutants (Figure 2B). Although wild-type E50 antibodies 1056 and 1534 bound well to AE.A244 gp120 and the AE.A244 V1V2 tag subunit protein, binding was lost or greatly diminished to these antigens in the E50K reverted antibodies (Figure 2B). Additionally, neutralization of the tier 1 HIV-1 strain C.MW965.26 was substantially reduced for 1534 E50K and lost for 1056 E50K (Figure 2C), demonstrating that acquisition of the ED motif resulted in the gain of heterologous tier 1 HIV-1 neutralization capacity.

Limited Availability of LCDR2 ED Motif in the Antibody Repertoires of Humans and Rhesus Macaques

Thus, 71% (29/41) of the total number of V2 antibodies and 58% (15/26) of the V2-reactive clonal lineages isolated from three rhesus macaque Env immunization studies bound at K169, and all 29 K169-recognizing antibodies included the CDRL2 ED motif either by using *IGLV3-17* in which ED is germline encoded (27 MAbs), or by acquiring ED through somatic mutations (2 MAbs) (Figure 3). Given the remarkable usage of the ED motif for K169 recognition in both the human and rhesus immune response to HIV-1 Env immunization, we next asked how frequently the LCDR2 ED motif is encoded in the human and rhesus macaque light chain repertoires.

In humans, the LCDR2 ED motif is encoded in three V_λ gene segments: *IGLV3-10*, *IGLV6-57*, and *IGLV3-22*. *IGLV3-22* has two alleles: *IGLV3-22*02* is a pseudogene with a frame-shift mutation producing a premature stop codon and *IGLV3-22*01* is potentially functional (Frippiat and Lefranc, 1994; Lefranc, 2001). *IGLV3-22* has not, however, been observed in lambda rearrangements in GenBank antibody sequences, suggesting that the dominant allele is *IGLV3-22*02* that effectively restricts germline encoding of the ED motif in the human repertoire to two light chain V_λ gene segments, *IGLV6-57* and *IGLV3-10*. These two gene segments were precisely those utilized by the

A

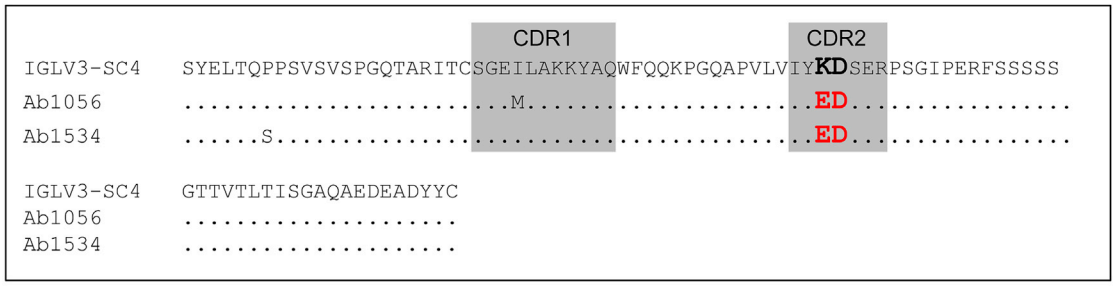

B

	ELISA Binding EC50 (ug/ml)			
	Ab1056		Ab1534	
Antigen	WT	E50K Mut	WT	E50K Mut
CAP206 T/F gp140	0.006	0.026	0.009	0.055
A244 gp120	0.129	>100	0.096	26.664
A244 V1V2 Tags	0.016	33.621	0.013	30.923

C

Antibody	MW965.26 (IC50 ug/ml)
1056 WT	18.9
1056 E50K Mut	>50
1534 WT	14.4
1534 E50K Mut	28.1

Figure 2. CDRL2 ED Motif Can Be Acquired by Affinity Maturation

(A) Amino acid sequence alignment of V_L region of antibodies 1056 and 1534 to their inferred germline V_L gene segment. IGLV3-SC4 shows that K50E somatic hypermutation confers the ED motif (red). Dots represent amino acid matches to germline. The ED motif is bolded for emphasis.

(B) ELISA binding results for clonally related WT antibodies 1056 and 1534 and reverted E50K mutants tested against CAP206 (autologous) and A244 antigens.

(C) Neutralization of clade C tier 1 MW965.26 in TZM-bl cell assay (orange denotes neutralization at <50 μg/ml).

Data are from one experiment (B and C) with neutralization values (C) representing the average of duplicate measurements.

human V2 K169 antibodies isolated from RV144 vaccinees (n = 4) (Liao et al., 2013).

The known rhesus macaque light chain repertoire includes only two light chain V gene segments that encode for the LCDR2 ED motif in the germline, *IGLV3-17* and *IGLV3-30*. Rhesus *IGLV3-17* is an ortholog of human *IGLV3-10* and the gene segments share 97% sequence similarity (Figure 4, Table S4). *IGLV3-30* is an ortholog of human *IGLV3-22*. As with human *IGLV3-22*, no *IGLV3-30* antibodies have been observed in GenBank. However, the incomplete characterization of rhesus Ig gene segments prevents us from establishing whether nonfunctional alleles for this gene segment exist. The rhesus ortholog of human *IGLV6-57* is *IGLV6-92*, but *IGLV6-92* encodes for a KD in its LCDR2. It is important to note that characterization of the rhesus Ig gene segment repertoire is incomplete, and it is possible that more gene segments or alleles that include an ED motif in the LCDR2 might be defined in the future.

Conservation of the *IGLV3-10* V Gene Segment in Primate Phylogeny

Because we have observed antibodies containing the LCDR2 ED motif in both human and rhesus antibody responses to HIV-1 V2 K169 and found that the ED motif is encoded in the germline V_λ segments of both species, we next asked whether the ED motif is present in the V_λ gene segments of other primates. We searched for all human *IGLV3-10* orthologs within 12 primate genomes. The genomes queried consisted of a diverse set of primates including representatives from the groups of great apes, old world monkeys, new world monkeys, tarsiers, and lemurs. All 12 primate genomes contained *IGLV3-10* orthologs and in all but two (*Pongo abelii* and *Saimiri boliviensis*), the LCDR2 ED motif was present within their respective *IGLV3-10* ortholog (Figure 5A). Within great apes, bonobos, and old world monkeys, the orthologs are highly similar to human *IGLV3-10* with sequence identities greater than 95% (Figure 5B). Sequence identities of orthologs in the more distant extant primate groups of new world monkeys, tarsiers, and lemurs are between 84% and 89%. Rhesus macaque and humans shared a common ancestor an estimated 32 million years ago (Perelman et al., 2011), demonstrating that the *IGLV3-10* gene segment has not been altered substantially and has maintained the ED motif over that time period (Figure 5B). Given the presence of the ED motif in the mouse lemur (*Microcebus murinus*) light chain repertoire, the conservation of the ED motif in the primate lineage can be traced as far back as an estimated 87 million years ago (Perelman et al., 2011). The ED motifs in the *IGLV3-10* primate orthologs are

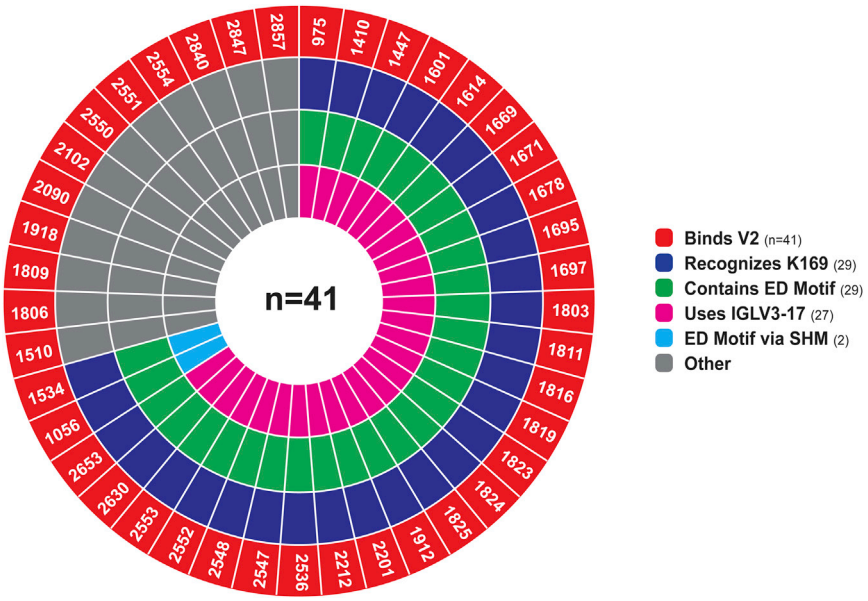

Figure 3. All K169-Dependent V2 Antibodies Contain the CDRL2 ED Motif

Summary of characteristics of the rhesus antibodies. Antibody names are labeled in the segments of the outer ring for antibodies with V2-binding reactivity (red). Segments proceeding inward toward center indicate additional characteristics of the antibody. The first inner ring specifies K169-dependent V2 recognition (blue) and second inner ring specifies presence of LCDR2 ED motif (green). The innermost ring specifies IGLV3-17 germline usage (magenta) or ED motif gained by somatic hypermutation (SHM) (cyan). Gray segments denote antibodies without the specified characteristic at that ring level. Data are representative of two independent experiments for purified antibodies and one experiment for antibodies from initial primary screening (see Table S1 for breakdown).

encoded by several different combinations of codon pairs (Figure S3) with heterogeneity in codon usage observed in the more distant primate species from human, providing further evidence of a strong selective pressure for maintenance of the ED motif.

Structural Insights into Germline IGLV3-10 Usage and K169 Recognition

In order to gain structural insights into IGLV3-10 usage and V2 K169 recognition, we determined the crystal structure of the CH59 unmutated ancestor (CH59-UA) antibody that utilizes the germline IGLV3-10 segment (Figure 6A, Table S5). CH59-UA binds with micromolar affinity to the AE.A244 V2 peptide (K_d = 0.5 μM), a value two orders of magnitude weaker than the affinity of the mutated CH59 antibody (K_d = 3.1 nM) (Figure S4). Superposition of the CH59-UA structure onto the structure of mature CH59 in complex with a V2 peptide (Liao et al., 2013) revealed that the CH59 V2 K169 binding site is remarkably similar to the corresponding paratope of CH59-UA (Figure 6B). The average backbone root mean square deviation (rmsd) of the six CDRs was 1.26Å with the light chain CDRs aligning more closely (0.88Å rmsd) than the heavy chain CDRs (1.52Å rmsd). Particularly striking was the structural similarity between the respective ED motif conformations in the unliganded CH59-UA and the bound mature CH59. The CH59-UA E50 and D51 side chains are positioned in nearly identical orientations as the bound conformations of the corresponding side-chains in the mature CH59, demonstrating in an unliganded and germline IGLV3-10 antibody that the ED motif is in precisely the orientation used for recognizing K169 V2. Taken together, these data show that the CH59 binding site is largely preconfigured in the unliganded CH59-UA. Preconfiguration of an antibody binding site can mitigate the entropic penalty paid upon association (Schmidt et al., 2013), and consistent with this prediction, the CH59-UA has a very fast on-rate (Figure S4). The on-rate of the CH59-UA was observed to be similar to that of the mature CH59 on-rate; consequently, affinity maturation in the CH59 lineage is driven by off-rate improvements. Given that rhesus IGLV3-17 has 97% sequence identity to human IGLV3-10, we expect that the germline structure of rhesus IGLV3-17 is probably identical to the structure of human IGLV3-10. Consequently, the light chain recognition mode of rhesus IGLV3-17 antibodies to the HIV-1 V2 K169 epitope must closely resemble light chain recognition in the CH59 antibody lineage.

All rhesus macaque V2 antibodies isolated that contain the ED motif have LCDR3 lengths of 11 residues (Table S2), the same length as the LCDR3 of the human RV144 trial vaccine antibody, CH59. We next asked how compatible the ED

```
                                          CDR1                          CDR2
Human  IGLV3-10   SYELTQPPSVSVSPGQTARITCSGDALPKKYAYWYQQKSGQAPVLVIYEDSKRPSGIPERFS
Rhesus IGLV3-17   ......................................F...P..S...I..............

Human  IGLV3-10   GSSSGTMATLTISGAQVEDEADYYC
Rhesus IGLV3-17   ......V..................
```

```
                                          CDR1                          CDR2
Human  IGLV6-57 NFMLTQPHSVSESPGKTVTISCTRSSGSIASNYVQWYQQRPGSSPTTVIYEDNQRPSGVPDRFS
Rhesus IGLV6-92 EVVF.......G...Q.....................D.E.....A......K..............

Human  IGLV6-57   GSIDSSSNSASLTISGLKTEDEADYYC
Rhesus IGLV6-92   ............A.....S........
```

Figure 4. Rhesus Orthologs of Human VLs Encoding for CDRL2 ED Motif in the Germline

Amino acid sequence alignments of the rhesus V_L orthologs to human IGLV3-10 and IGLV6-57. Dots represent amino acid residue matches. The ED motif is bolded and colored red for emphasis.

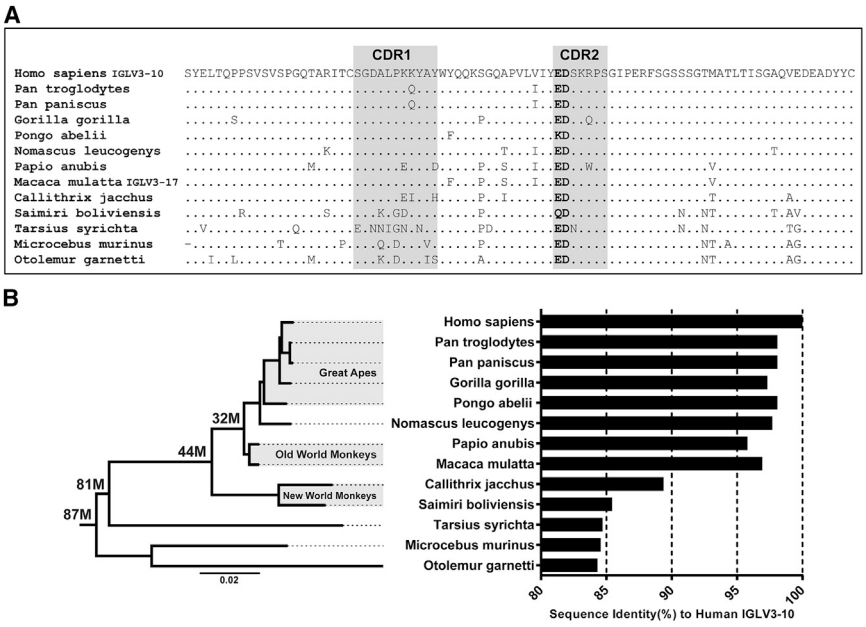

Figure 5. Conservation of IGLV3-10 and ED Motif in Primate Phylogeny

(A) Amino acid sequence alignment of human IGLV3-10 to orthologs from 12 primates with sequenced genomes. Dots represent amino acid residue matches and residues in the LCDR2 ED motif positions are bolded for emphasis.

(B) Sequence identities of primate IGLV3-10 orthologs to human IGLV3-10 (right) juxtaposed to phylogenetic tree including respective primate species (left). Data on estimated time (in millions of years ago) to most common recent ancestor (shown in bold on tree nodes for relevant estimates) as well as for phylogenetic tree were taken from Perelman et al. (2011). Branch length estimate units are substitution/site.

antibody sequences were with the CH59 structure in complex with V2 (Liao et al., 2013). We threaded the sequence of a representative ED motif-containing rhesus antibody, Ab975, onto the CH59-V2 peptide complex structure, and the structural model of Ab975 demonstrated agreement with the CH59 mode of V2 recognition (Figure S4E). The ED motif of Ab975 is predicted to adopt a similar orientation as CH59, suggesting that the ED motif of Ab975 could also form salt bridges with K169 and K171, which is consistent with the epitope mapping of Ab975 (Table 1). The binding pocket opposite the C-terminal half of the V2 peptide in the structural model of Ab975 is shallower than CH59's binding pocket, most likely reflecting differences in the heavy chain usage between Ab975 and CH59.

Analysis of Rhesus Macaque V_H Pairing with IGLV3-17 ED Antibodies

All IGLV3-17 ED-motif-containing antibodies shared the amino acid H173 in their V2 epitopes (Table 1). In the crystal structure of the complex of CH59 with a V2 peptide, the heavy chain contacted residues C-terminal of K169 with H173 forming hydrogen bond contacts with Asp 95 (D95) in the heavy chain (Liao et al., 2013). Although V_H pairing with IGLV3-17 does not appear to be overly restricted, with four distinct V_H gene segments used among 15 IGLV3-17 clones (Table S2), all IGLV3-17 antibodies isolated contained D95, like CH59 (Figure S5), suggesting that D95 might play a functional role in their V2 recognition. Because of the incomplete characterization at the 3′ end of V_H gene segments in the rhesus repertoire, we cannot be certain about the frequency in which D95 is encoded in heavy chains and whether this structural feature represents an additional restriction for recognition of the V2 epitope.

It is notable, however, that we have not observed the CH59 IGHV3-9 rhesus ortholog, IGHV3-78 (Table S4B), paired with the IGLV3-17 of the rhesus ED motif antibodies. We hypothesized that the lack of rhesus heavy and light chain pairs that were orthologous to the CH59 pairing could be due to incompatibly of the IGHV3-78 sequence in the CH59 V2 recognition mode. A structural model of IGHV3-78:IGLV3-17 in the CH59 recognition mode resulted in severe clashing between the Y59 residue in the HCDR2 and the V2 peptide (Figure S4F). In CH59, the *IGHV3-9* germline gene does not encode a large amino acid such as tyrosine but instead the smallest amino acid residue, glycine, which allows for favorable paratope shape complementarity with the V2 peptide. Thus, the steric hindrance of IGHV3-78 with the V2 peptide when structurally modeled into the CH59 recognition mode suggests a potential explanation for why we do not observe IGHV3-78:IGLV3-17 pairing in the rhesus V2 antibody response.

DISCUSSION

In this study, we demonstrate that the dominant antibody response in recognition of the V2 epitope surrounding lysine at amino acid position 169 in rhesus macaques utilizes the IGLV3-17 gene segment with a LCDR2 ED amino acid pair. We show that the V_L ED motif can arise either by being encoded in the *IGLV3-17* germline gene or arise in the course of somatic mutation from a germline-encoded KD LCDR2 motif. Remarkably, the rhesus *IGLV3-17* gene is the ortholog of the human *IGLV3-10* gene, which is utilized for recognition of the V2 K169 site in humans (Liao et al., 2013).

The rhesus IGLV3-17 ED motif antibodies had very similar neutralization profiles as human ED motif Abs CH58 and CH59, and rhesus ED motif Ab V2 footprints were most consistent with the V2 epitope of human V2 mAb CH59. The epitope footprints of human RV144 vaccinee V2 antibodies HG107 and HG120 were also similar to CH59, and all three antibodies used the IGLV3-10 gene segment, demonstrating that human IGLV3-10 and rhesus IGLV3-17 ortholog usage confers a highly consistent V2 recognition mode in both human and rhesus anti-V2 antibodies.

Of the four distinct V_H gene segments observed to pair with IGLV3-17, two pairings, IGHV4-48:IGLV3-17 and IGHV4-79:IGLV3-17, occurred independently in two monkeys given two different immunization regimens. In addition, one V_H:V_L

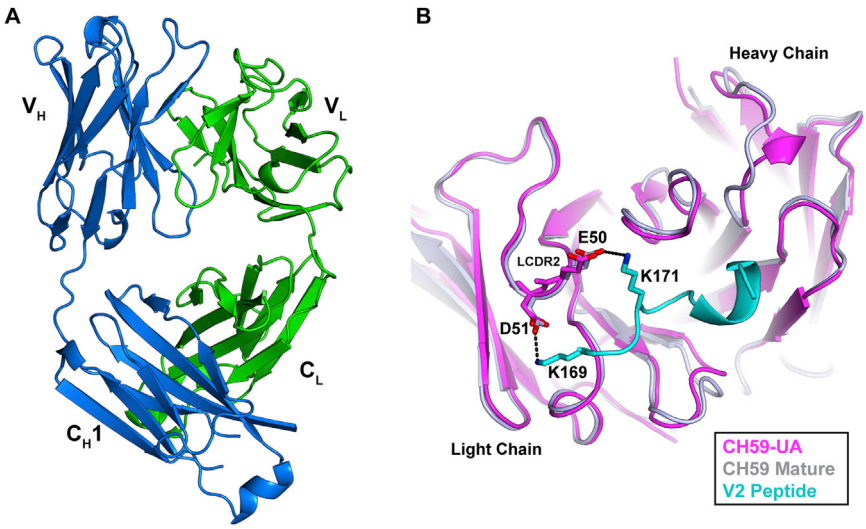

Figure 6. CH59-UA Structure Reveals Preconfigured K169 Recognition Mode in IGLV3-10 Germline

(A) Crystal structure of the CH59-UA Fab with heavy chain colored blue and light chain colored green. See Table S5 for summary of structural data.

(B) Superposition of crystal structures of CH59-UA (magenta) and mature CH59 (gray) in complex with a V2 peptide (cyan). The ED motif in CDRL2 of both antibodies and K169 and K171 of V2 peptide are shown in stick representation. Dashed lines indicate salt bridges in mature CH59-V2 complex.

pair, IGHV3-SC11:IGLV3-17, was the orthologous pairing of the K169-recognizing ED motif antibody HG120 isolated from an RV144 subject. These data demonstrated that although there are many solutions to the problem of epitope recognition, the antibody response can enlist common modes of recognition through preferential V_H:V_L pairing. Although V_H:V_L pairing is thought to be largely a stochastic process (de Wildt et al., 1999; Jayaram et al., 2012), the selection process itself is not random and those pairings that result in high-affinity binding of antigen by the naive BCR will be preferentially selected (Dal Porto et al., 1998; Shih et al., 2002). In HIV-1 infection, restricted pairing among different individuals has previously been reported for the VRC-01 CD4 binding site class of bnAbs where IGHV1-2 or IGHV1-46 must pair with light chain VJ rearrangements with a very short LCDR3 (West et al., 2012) in order to mimic CD4 in binding to the gp120 CD4 binding site at the correct angle for broad neutralization (Zhou et al., 2013). An additional example of restricted pairing in the HIV-1 antibody response is the V_H:V_L pairing of IGHV1-69:IGKV3-20, which has been observed for two gp41 neutralizing antibodies, 4E10 and CAP206-CH12 (Morris et al., 2011; Zwick et al., 2001), that recognize a similar MPER epitope. Unlike in broadly neutralizing HIV-1 antibodies (Haynes et al., 2012b), the ED motif antibodies have low levels of somatic mutations. Therefore, although the ED motif-containing antibodies are associated to date with a low level of vaccine efficacy (Haynes et al., 2012a; Liao et al., 2013; Rerks-Ngarm et al., 2009), they are readily inducible, making the ED antibody response a desirable type of vaccine-induced response. One problem with the RV144 vaccine response was the limited breadth of the V2 response (Rolland et al., 2012). Efforts to broaden the V2 response with more V2 immunogen motifs will be one key to improving vaccine efficacy.

Several conformational V2 antibodies with limited neutralization have been elicited in HIV-1 infection and described previously (Gorny et al., 1994, 2012; Mayr et al., 2013). Analysis of one of these antibodies, 697-D, demonstrated that unlike CH58 and CH59, V2 binding was not dependent on K169 (Liao et al., 2013). Additional analysis of published binding data of six additional infection-derived V2 antibodies showed that none of the conformational V2 antibodies were K169 sensitive (Gorny et al., 2012). Thus, although infection-derived V2 antibodies represent a class of V2 antibodies, they do not share the same recognition properties as the human or rhesus V2 ED-motif-dependent antibodies elicited from vaccination.

It is important to note that ED-motif-bearing antibodies target the V2 loop at K169 that is also a component of the V1V2-glycan epitope recognized by the PG9 class of broadly neutralizing antibodies comprised of PG9, PG16, CAP256-VRC26, and CH01 (Kwong and Mascola, 2012). This class of bnAbs is characterized by their extremely long HCDR3s (24–37 amino acids in length), sulfated tyrosines by posttranslational modification, and recognition of glycans in the V2 loop. The pool of B cells with extremely long CDRs is thought to be very small with <1% of B cells of HCDR3s greater than 28 (Briney et al., 2012). In addition, a tyrosine within a larger amino acid motif is required for sulfation to occur (Stone et al., 2009). Taken together, the low likelihood of these bnAb requirements occurring simultaneously could help explain the difficulty of eliciting this type of bnAb response. The observation that ED motif antibodies target a linear V2 epitope and are easy to induce could also act to block elicitation of PG9-class bnAbs.

Finally, recent estimates have placed primate lentivirus infection occurring as long as 12 million years ago (Compton and Emerman, 2013), and lysine at position 169 is relatively well conserved in Envs of simian immunodeficiency virus strains infecting many primate species (HIV/SIV Sequence Database http://www.hiv.lanl.gov/content/index). The observation that IGLV3-10 has highly similar orthologs throughout the primate lineage that include the ED motif suggests that the ED motif probably confers an evolutionary advantage within the antibody response. One hypothesis is that a recent evolutionary driving factor for ED motif maintenance could be primate retroviral defense.

EXPERIMENTAL PROCEDURES

Immunization of Rhesus Macaques

Rhesus macaque immunization regimens for NHP studies 36, 54, and 62.1 are summarized in Figure S1. For NHP study 36, immunizations were given intramuscularly five times at weeks 0, 4, 12, 23, and 53 at 5×10^7 pfu per dose of ALVAC and 600 μg per dose of AIDSVAX B/E gp120 (five rhesus macaques). Blood, spleen, and terminal ileum, as well as mesenteric, inguinal, anterior

pelvic, posterior pelvic, and periaortic lymph node samples were collected at 2 weeks after the fifth immunization. For NHP study 54, immunizations were given intramuscularly seven times at 6 week intervals with 100 μg per dose (six rhesus macaques). Blood samples were collected at 2 weeks after the third immunization. For NHP study 62.1, immunizations were given intramuscularly five times at 6 week intervals with 100 μg per dose (six rhesus macaques). Blood samples were collected at 2 weeks after the fifth immunization. All rhesus macaques were housed at Bioqual (NHP studies 54 and 62.1) and the New England Primate Research Center, Southborough, MA (NHP study 36). All rhesus macaques were maintained in accordance with the Association for Assessment and Accreditation of Laboratory Animals with the approval of the Animal Care and Use Committees of the National Institutes of Health and Harvard Medical School. Research was conducted in compliance with the Animal Welfare Act and other federal statutes and regulations relating to animals and experiments involving animals and adheres to principles stated in the Guide for the Care and Use of Laboratory Animals, NRC Publication, 2011 edition.

Antibody Isolation

AE.A244 gp120D11 and AE.A244 V1V2 peptides were conjugated with either AF647 or BV421 (Invitrogen) dyes. Protein quality after conjugations was assessed by flow cytometry for binding to a panel of well-characterized HIV-1-specific antibodies. Peripheral blood mononuclear cells (PBMCs) of immunized rhesus macaques were stained with AquaVital dye, CD14 (BV570), CD16 (PE-Cy7), CD3 (PerCP Cy5.5), CD20 (FITC), CD27 (APC-Cy7), and IgD (PE). Antigen-specific memory B cells were single-cell sorted with a BD FACS Aria II into 96-well plates containing 20 μl of reverse transcriptase buffer (RT) by gating on AquaVital dye$^-$, CD14$^-$, CD16$^-$, CD3$^-$, IgD$^-$, CD20$^+$, CD27$^+$, BV421 and AF647 double-positive cells. Immunoglobulin (Ig) heavy and light chain genes (VH and VL) were PCR amplified via a modified version of a previously described protocol (Liao et al., 2009), optimized for the amplification of rhesus antibodies (R.Z., unpublished data). The RT reaction was performed with 0.100 μM of constant region primers IgG, IgM, IgA, IgD, IgE, Igκ, and Igλ (Table S6). Primers and RNA were first incubated at 65°C for 5 min. The PCR plate was chilled to 4°C and 0.75 mM dNTPs (QIAGEN), SSIII (U) (Invitrogen), and RNase Out (U) (Invitrogen) was added followed by an incubation at 50°C for 45 min, 55°C for 15 min. The cDNA was then amplified with two PCR steps. In the first step, 5 μl of cDNA, 10× PCR Buffer (QIAGEN), 10× Q Buffer (QIAGEN), 0.20 mM dNTPs (QIAGEN), $MgCl_2$ (IgH 0.50 mM, Igκ 1.00 mM, Igλ 1.50 mM), and 0.125 μM of either IgA1, IgA2, IgD, IgG, IgM, or Igκ, or Igλ with IgH, Igκ, or Igλ variable region primers (Table S6) were PCR amplified in a 50 μl reaction at 95°C for 5 min, 94°C for 30 s, 64°C (Igκ and Igλ) or 62°C (IgH) for 45 s, 72°C for 90 s for 35 cycles followed by one cycle of 72°C for 7 min for IgH. Nested PCR was then performed in individual amplifications with 3.0 μl of PCR product, 10× PCR Buffer (QIAGEN), 10× Q Buffer (QIAGEN), 0.20 mM dNTPs (QIAGEN), $MgCl_2$ (IgH 1.50 mM, Igκ 1.00 mM, Igλ 1.00 mM), with 0.500 μM of IgH, or Igκ, or Igλ internal forward and reverse variable region primers (Table S6). The nested PCR conditions were: 95°C for 5 min, 94°C for 30 s, 64°C (Igκ and Igλ) or 62°C (IgH) for 45 s, 72°C for 90 s for 35 cycles followed by one cycle of 72°C for 7 min. PCR products were analyzed on 1.2% SYBER Safe E-Gels (Invitrogen). VH and VL PCR-amplified genes were then purified and sequenced, sequences were analyzed, and VDJ arrangements were inferred with previously described computational methods (Kepler, 2013; Munshaw and Kepler, 2010).

Transient and Recombinant Antibody Expression

Transient and recombinant antibody expressions were performed as previously described (Liao et al., 2009, 2011).

ELISA

ELISA assays were performed as previously described (Liao et al., 2011). K169 sensitivity in the initial screen of transient transfected V2 antibodies was established with ELISA by computing the area under the curve (AUC) for three serial dilutions (1:1, 1:3, and 1:9) for antibody binding to wild-type 171 V2 peptide and the K169A 171. Antibodies for which >50% reduction in K169A AUC relative to WT was observed were classified as K169 dependent. For epitope mapping of purified antibodies, ELISA half-maximal effective concentrations (EC_{50}s) were calculated by curve fitting via a five parameter logistic model and epitope positions defined by V2 171 peptide alanine scan mutations that reduced EC_{50}s by >50% relative to wild-type. Site-directed mutagenesis was performed as previous described (Gao et al., 2014).

Neutralization Assays

Neutralization activity of antibodies was measured in TMZ-bl cell-based (Sarzotti-Kelsoe et al., 2014) and A3R5.7 cell-based (McLinden et al., 2013) neutralization assays.

SPR Kinetics Measurements

Epitope mapping experiments in SPR were performed on a BIAcore 4000 (BIAcore) instrument at 25°C. Using a Series S CM5 chip, wild-type and ala-substituted peptides were amine-coupled directly on the chip surface. Data analyses were performed with the Biacore 4000 evaluation and BIAevaluation 4.1 software (BIAcore) as previously described (Alam et al., 2007, 2011). Binding responses of the irrelevant respiratory syncytial virus (RSV) antibody Synagis was used to subtract out responses resulting from nonspecific interactions. Antibodies 1056 and 1534 failed to bind the AE.A244 171 peptide in ELISA assays but binding was detected with SPR and alanine scanning mutagenesis SPR was used to fine map the 1056 and 1534 epitopes with an epitope inclusion criteria of >50% reduction in SPR response units relative to wild-type peptide.

Sequence Analysis and Molecular Modeling

Details of the sequence analysis and molecular modeling performed are provided in the Supplemental Experimental Procedures.

Biolayer Interferometry Measurements

All biolayer interferometry (BLI) measurements were made with a ForteBio OctetRed 96 instrument and streptavidin sensors at 25°C and data analyses were performed with ForteBio data analysis 7 software. The $gp120_{165\text{-}182}$ peptide sensors were prepared by dipping streptavidin sensors into wells containing biotinlyated $gp120_{165\text{-}182}$ peptides (5 μg/ml) for 300 s. The peptide-loaded sensors were washed in PBS buffer (pH 7.4) for 60 s before obtaining baseline. The affinity measurements of the mature and UA Fabs of CH59 to the $gp120_{165\text{-}182}$ peptide were carried out by performing binding titrations (Fab concentrations ranged from 1 to 50 μg/ml). The gp41 MPER-specific 13H11 Fab (1–20 μg/ml) binding to the WT peptide sensors was used in parallel to subtract out binding resulting from nonspecific interactions with the sensors. The subtracted binding curves were fitted globally to a 1:1 binding model to obtain association (k_a) and dissociation (k_d) rate constants and the apparent dissociation constant (K_d). The titrations were performed in triplicate.

Crystallographic Analysis of CH59-UA

Fab fragments of CH59-UA were produced recombinantly as previously described (Nicely et al., 2010). In short, Fab chains were generated by PCR with light and heavy chain genes as templates with appropriate primer pairs, and cloned into pcDNA3.1/hygro (Liao et al., 2006). Recombinant Fabs were produced in 293F cells by cotransfection with heavy chain and light chain gene plasmids, then purified via the methods described previously (Nicely et al., 2010). After affinity capture with CaptureSelect Fab lambda affinity matrix [BAC] under standard conditions, the Fab was further purified via gel filtration chromatography with a HiLoad 26/60 Superdex 200pg 26/60 column at 2 ml/min with a buffer of 10 mM HEPES (pH 7.2), 50 mM NaCl, 0.02% NaN_3. Fab peak elution fractions were pooled and exchanged into ddH_2O via five dilute/concentrate cycles and brought to a final concentration of 15.0 mg/ml.

Unliganded Fab was tested in various crystallization screens in SBS format with reservoir volumes of 60 μl and drop volumes of 0.6 μl. Plates were incubated at 20°C. Crystals of CH59-UA were observed over a reservoir of 0.05 M calcium chloride dihydrate, 0.1 M MES monohydrate (pH 6.0), 45% PEG 200 in drops composed of 0.3 μl protein + 0.3 μl reservoir with the protein solution at 15 mg/ml. These crystals were cryo-cooled directly from the drop.

Data on the crystal was collected at SER-CAT BM with an incident beam with wavelength of 1 Å. Data were reduced in HKL-2000 (Otwinowski and Minor, 1997). Matthews analysis suggested two Fabs in the asymmetric unit of the unliganded CH59-UA structure (Matthews, 1968). The structure was phased by molecular replacement in PHENIX (Terwilliger et al., 2008) with as the source model the mature CH59 Fab structure (Liao et al., 2013). Rebuilding

and real-space refinements were done in Coot (Emsley et al., 2010) with reciprocal space refinements in PHENIX (Adams et al., 2010) and validations in MolProbity (Lovell et al., 2003). The crystal structure of unliganded CH59-UA Fab was refined to a resolution of 2.4 Å (Table S1).

ACCESSION NUMBERS

The GenBank accession numbers for V_H and V_L sequences of the rhesus antibodies reported in this paper are KJ956810–KJ956891. Coordinates and structure factors for CH59-UA have been deposited into the Protein Data Bank with accession code 4QF1.

SUPPLEMENTAL INFORMATION

Supplemental Information includes five figures, six tables, and Supplemental Experimental Procedures and can be found with this article online at http://dx.doi.org/10.1016/j.immuni.2014.11.014.

AUTHOR CONTRIBUTIONS

D.E., K.L., and T.B. isolated antibodies, designed assays, and analyzed data. K.W. conducted structural and sequence analyses, data analyses, and interpretation. K.W. and D.E. edited the manuscript. N.I.N. performed structural analysis of CH59. F.H.J., S.M.D., and S.M.A. performed protein purification and SPR assays. R.Z. and H.-X.L. contributed to rhesus PCR and antibody production. K.E.L., C.S., and R.P. performed antibody binding assays. L.L.S., R.M.S., and S.S. performed rhesus immunizations. L.M. provided CAP206 Envs and sequences. J.K., S.N., P.P., S.R.-N., N.L.M., and J.H.K. provided vaccine. G.K. and M.B. provided experimental design and interpreted data. D.C.M. performed neutralization assays. G.D.T. performed antibody binding assays. T.B.K. designed software and performed computational analyses of antibody sequences and inferred UCAs. M.A.M. produced fluorophor-labeled Env proteins for memory B cell cultures, and B.F.H. designed the study, oversaw all experiments, and analyzed all data. K.W. and B.F.H. wrote the paper.

ACKNOWLEDGMENTS

This work was supported by Collaboration for AIDS Vaccine Discovery grants from the Bill & Melinda Gates Foundation (grant ID OPP1033098) and by the Center for HIV/AIDS Vaccine Immunology-Immuongen Discovery (CHAVI-ID; UMI-AI100645) grant from NIH/NIAID/DAIDS. This work was also supported by grant number 5T32-AI007392 from the NIAID (NIH). Flow cytometry work was additionally supported by The Duke University Center for AIDS Research Flow Cytometry core (NIAID, NIH, CFAR grant P30-AI-64518). Funding was also provided by Interagency Agreement Y1-AI-2642-12 between U.S. Army Medical Research and Material Command (USAMRMC) and the National Institute of Allergy and Infectious Diseases through a cooperative agreement (W81XWH-07-2-0067) between the Henry M. Jackson Foundation for the Advancement of Military Medicine, Inc., and the U.S. Department of Defense (DOD). The views expressed in this article are those of the authors and should not be construed as official or as representing the views of the Department of Defense or the Department of the Army. Use of the Advanced Photon Source was supported by the U.S. Department of Energy, Office of Science, Office of Basic Energy Sciences, under Contract No. W-31-109-Eng-38. We thank A. Foulger for expert technical assistance in antibody production; D. Marshall and J. Whitesides for expert technical assistance in flow cytometry; A. Martelli for expert technical assistance in neutralization assays; and K. Soderberg and S. Bowen for project management.

Received: June 3, 2014
Accepted: October 20, 2014
Published: December 18, 2014

REFERENCES

Adams, P.D., Afonine, P.V., Bunkóczi, G., Chen, V.B., Davis, I.W., Echols, N., Headd, J.J., Hung, L.W., Kapral, G.J., Grosse-Kunstleve, R.W., et al. (2010). PHENIX: a comprehensive Python-based system for macromolecular structure solution. Acta Crystallogr. D Biol. Crystallogr. *66*, 213–221.

Alam, S.M., McAdams, M., Boren, D., Rak, M., Scearce, R.M., Gao, F., Camacho, Z.T., Gewirth, D., Kelsoe, G., Chen, P., and Haynes, B.F. (2007). The role of antibody polyspecificity and lipid reactivity in binding of broadly neutralizing anti-HIV-1 envelope human monoclonal antibodies 2F5 and 4E10 to glycoprotein 41 membrane proximal envelope epitopes. J. Immunol. *178*, 4424–4435.

Alam, S.M., Liao, H.X., Dennison, S.M., Jaeger, F., Parks, R., Anasti, K., Foulger, A., Donathan, M., Lucas, J., Verkoczy, L., et al. (2011). Differential reactivity of germ line allelic variants of a broadly neutralizing HIV-1 antibody to a gp41 fusion intermediate conformation. J. Virol. *85*, 11725–11731.

Bonsignori, M., Pollara, J., Moody, M.A., Alpert, M.D., Chen, X., Hwang, K.K., Gilbert, P.B., Huang, Y., Gurley, T.C., Kozink, D.M., et al. (2012). Antibody-dependent cellular cytotoxicity-mediating antibodies from an HIV-1 vaccine efficacy trial target multiple epitopes and preferentially use the VH1 gene family. J. Virol. *86*, 11521–11532.

Briney, B.S., Willis, J.R., and Crowe, J.E., Jr. (2012). Human peripheral blood antibodies with long HCDR3s are established primarily at original recombination using a limited subset of germline genes. PLoS ONE *7*, e36750.

Compton, A.A., and Emerman, M. (2013). Convergence and divergence in the evolution of the APOBEC3G-Vif interaction reveal ancient origins of simian immunodeficiency viruses. PLoS Pathog. *9*, e1003135.

Dal Porto, J.M., Haberman, A.M., Shlomchik, M.J., and Kelsoe, G. (1998). Antigen drives very low affinity B cells to become plasmacytes and enter germinal centers. J. Immunol. *161*, 5373–5381.

de Wildt, R.M., Hoet, R.M., van Venrooij, W.J., Tomlinson, I.M., and Winter, G. (1999). Analysis of heavy and light chain pairings indicates that receptor editing shapes the human antibody repertoire. J. Mol. Biol. *285*, 895–901.

Emsley, P., Lohkamp, B., Scott, W.G., and Cowtan, K. (2010). Features and development of Coot. Acta Crystallogr. D Biol. Crystallogr. *66*, 486–501.

Frippiat, J.P., and Lefranc, M.P. (1994). Genomic organisation of 34 kb of the human immunoglobulin lambda locus (IGLV): restriction map and sequences of new V lambda III genes. Mol. Immunol. *31*, 657–670.

Gao, F., Bonsignori, M., Liao, H.X., Kumar, A., Xia, S.M., Lu, X., Cai, F., Hwang, K.K., Song, H., Zhou, T., et al. (2014). Cooperation of B cell lineages in induction of HIV-1-broadly neutralizing antibodies. Cell *158*, 481–491.

Gibbs, R.A., Rogers, J., Katze, M.G., Bumgarner, R., Weinstock, G.M., Mardis, E.R., Remington, K.A., Strausberg, R.L., Venter, J.C., Wilson, R.K., et al.; Rhesus Macaque Genome Sequencing and Analysis Consortium (2007). Evolutionary and biomedical insights from the rhesus macaque genome. Science *316*, 222–234.

Gnanakaran, S., Daniels, M.G., Bhattacharya, T., Lapedes, A.S., Sethi, A., Li, M., Tang, H., Greene, K., Gao, H., Haynes, B.F., et al. (2010). Genetic signatures in the envelope glycoproteins of HIV-1 that associate with broadly neutralizing antibodies. PLoS Comput. Biol. *6*, e1000955.

Gorny, M.K., Moore, J.P., Conley, A.J., Karwowska, S., Sodroski, J., Williams, C., Burda, S., Boots, L.J., and Zolla-Pazner, S. (1994). Human anti-V2 monoclonal antibody that neutralizes primary but not laboratory isolates of human immunodeficiency virus type 1. J. Virol. *68*, 8312–8320.

Gorny, M.K., Pan, R., Williams, C., Wang, X.H., Volsky, B., O'Neal, T., Spurrier, B., Sampson, J.M., Li, L., Seaman, M.S., et al. (2012). Functional and immunochemical cross-reactivity of V2-specific monoclonal antibodies from HIV-1-infected individuals. Virology *427*, 198–207.

Haynes, B.F., Gilbert, P.B., McElrath, M.J., Zolla-Pazner, S., Tomaras, G.D., Alam, S.M., Evans, D.T., Montefiori, D.C., Karnasuta, C., Sutthent, R., et al. (2012a). Immune-correlates analysis of an HIV-1 vaccine efficacy trial. N. Engl. J. Med. *366*, 1275–1286.

Haynes, B.F., Kelsoe, G., Harrison, S.C., and Kepler, T.B. (2012b). B-cell-lineage immunogen design in vaccine development with HIV-1 as a case study. Nat. Biotechnol. *30*, 423–433.

Jayaram, N., Bhowmick, P., and Martin, A.C. (2012). Germline VH/VL pairing in antibodies. Protein Eng. Des. Sel. *25*, 523–529.

Kepler, T.B. (2013). Reconstructing a B-cell clonal lineage. I. Statistical inference of unobserved ancestors. F1000Res. *2*, 103.

Kwong, P.D., and Mascola, J.R. (2012). Human antibodies that neutralize HIV-1: identification, structures, and B cell ontogenies. Immunity *37*, 412–425.

Lefranc, M.P. (2001). IMGT, the international ImMunoGeneTics database. Nucleic Acids Res. *29*, 207–209.

Liao, H.X., Sutherland, L.L., Xia, S.M., Brock, M.E., Scearce, R.M., Vanleeuwen, S., Alam, S.M., McAdams, M., Weaver, E.A., Camacho, Z., et al. (2006). A group M consensus envelope glycoprotein induces antibodies that neutralize subsets of subtype B and C HIV-1 primary viruses. Virology *353*, 268–282.

Liao, H.X., Levesque, M.C., Nagel, A., Dixon, A., Zhang, R., Walter, E., Parks, R., Whitesides, J., Marshall, D.J., Hwang, K.K., et al. (2009). High-throughput isolation of immunoglobulin genes from single human B cells and expression as monoclonal antibodies. J. Virol. Methods *158*, 171–179.

Liao, H.X., Chen, X., Munshaw, S., Zhang, R., Marshall, D.J., Vandergrift, N., Whitesides, J.F., Lu, X., Yu, J.S., Hwang, K.K., et al. (2011). Initial antibodies binding to HIV-1 gp41 in acutely infected subjects are polyreactive and highly mutated. J. Exp. Med. *208*, 2237–2249.

Liao, H.X., Bonsignori, M., Alam, S.M., McLellan, J.S., Tomaras, G.D., Moody, M.A., Kozink, D.M., Hwang, K.K., Chen, X., Tsao, C.Y., et al. (2013). Vaccine induction of antibodies against a structurally heterogeneous site of immune pressure within HIV-1 envelope protein variable regions 1 and 2. Immunity *38*, 176–186.

Lovell, S.C., Davis, I.W., Arendall, W.B., 3rd, de Bakker, P.I., Word, J.M., Prisant, M.G., Richardson, J.S., and Richardson, D.C. (2003). Structure validation by Calpha geometry: phi,psi and Cbeta deviation. Proteins *50*, 437–450.

Matthews, B.W. (1968). Solvent content of protein crystals. J. Mol. Biol. *33*, 491–497.

Mayr, L.M., Cohen, S., Spurrier, B., Kong, X.P., and Zolla-Pazner, S. (2013). Epitope mapping of conformational V2-specific anti-HIV human monoclonal antibodies reveals an immunodominant site in V2. PLoS ONE *8*, e70859.

McLinden, R.J., Labranche, C.C., Chenine, A.L., Polonis, V.R., Eller, M.A., Wieczorek, L., Ochsenbauer, C., Kappes, J.C., Perfetto, S., Montefiori, D.C., et al. (2013). Detection of HIV-1 neutralizing antibodies in a human $CD4^+$/$CXCR4^+$/$CCR5^+$ T-lymphoblastoid cell assay system. PLoS ONE *8*, e77756.

Morris, L., Chen, X., Alam, M., Tomaras, G., Zhang, R., Marshall, D.J., Chen, B., Parks, R., Foulger, A., Jaeger, F., et al. (2011). Isolation of a human anti-HIV gp41 membrane proximal region neutralizing antibody by antigen-specific single B cell sorting. PLoS ONE *6*, e23532.

Munshaw, S., and Kepler, T.B. (2010). SoDA2: a Hidden Markov Model approach for identification of immunoglobulin rearrangements. Bioinformatics *26*, 867–872.

Nicely, N.I., Dennison, S.M., Spicer, L., Scearce, R.M., Kelsoe, G., Ueda, Y., Chen, H., Liao, H.X., Alam, S.M., and Haynes, B.F. (2010). Crystal structure of a non-neutralizing antibody to the HIV-1 gp41 membrane-proximal external region. Nat. Struct. Mol. Biol. *17*, 1492–1494.

Otwinowski, Z., and Minor, W. (1997). Processing of X-ray diffraction data collected in oscillation mode. Methods Enzymol. *276*, 307–326.

Perelman, P., Johnson, W.E., Roos, C., Seuánez, H.N., Horvath, J.E., Moreira, M.A., Kessing, B., Pontius, J., Roelke, M., Rumpler, Y., et al. (2011). A molecular phylogeny of living primates. PLoS Genet. *7*, e1001342.

Rerks-Ngarm, S., Pitisuttithum, P., Nitayaphan, S., Kaewkungwal, J., Chiu, J., Paris, R., Premsri, N., Namwat, C., de Souza, M., Adams, E., et al.; MOPH-TAVEG Investigators (2009). Vaccination with ALVAC and AIDSVAX to prevent HIV-1 infection in Thailand. N. Engl. J. Med. *361*, 2209–2220.

Rolland, M., Edlefsen, P.T., Larsen, B.B., Tovanabutra, S., Sanders-Buell, E., Hertz, T., deCamp, A.C., Carrico, C., Menis, S., Magaret, C.A., et al. (2012). Increased HIV-1 vaccine efficacy against viruses with genetic signatures in Env V2. Nature *490*, 417–420.

Sarzotti-Kelsoe, M., Bailer, R.T., Turk, E., Lin, C.L., Bilska, M., Greene, K.M., Gao, H., Todd, C.A., Ozaki, D.A., Seaman, M.S., et al. (2014). Optimization and validation of the TZM-bl assay for standardized assessments of neutralizing antibodies against HIV-1. J. Immunol. Methods *409*, 131–146.

Schmidt, A.G., Xu, H., Khan, A.R., O'Donnell, T., Khurana, S., King, L.R., Manischewitz, J., Golding, H., Suphaphiphat, P., Carfi, A., et al. (2013). Preconfiguration of the antigen-binding site during affinity maturation of a broadly neutralizing influenza virus antibody. Proc. Natl. Acad. Sci. USA *110*, 264–269.

Shih, T.A., Meffre, E., Roederer, M., and Nussenzweig, M.C. (2002). Role of BCR affinity in T cell dependent antibody responses in vivo. Nat. Immunol. *3*, 570–575.

Stone, M.J., Chuang, S., Hou, X., Shoham, M., and Zhu, J.Z. (2009). Tyrosine sulfation: an increasingly recognised post-translational modification of secreted proteins. New Biotechnol. *25*, 299–317.

Terwilliger, T.C., Grosse-Kunstleve, R.W., Afonine, P.V., Moriarty, N.W., Zwart, P.H., Hung, L.W., Read, R.J., and Adams, P.D. (2008). Iterative model building, structure refinement and density modification with the PHENIX AutoBuild wizard. Acta Crystallogr. D Biol. Crystallogr. *64*, 61–69.

West, A.P., Jr., Diskin, R., Nussenzweig, M.C., and Bjorkman, P.J. (2012). Structural basis for germ-line gene usage of a potent class of antibodies targeting the CD4-binding site of HIV-1 gp120. Proc. Natl. Acad. Sci. USA *109*, E2083–E2090.

Zhou, T., Zhu, J., Wu, X., Moquin, S., Zhang, B., Acharya, P., Georgiev, I.S., Altae-Tran, H.R., Chuang, G.Y., Joyce, M.G., et al.; NISC Comparative Sequencing Program (2013). Multidonor analysis reveals structural elements, genetic determinants, and maturation pathway for HIV-1 neutralization by VRC01-class antibodies. Immunity *39*, 245–258.

Zwick, M.B., Labrijn, A.F., Wang, M., Spenlehauer, C., Saphire, E.O., Binley, J.M., Moore, J.P., Stiegler, G., Katinger, H., Burton, D.R., and Parren, P.W. (2001). Broadly neutralizing antibodies targeted to the membrane-proximal external region of human immunodeficiency virus type 1 glycoprotein gp41. J. Virol. *75*, 10892–10905.